

# The Cosmological Arrow of Time from Inflationary Branch Decoherence

Ali Nayeri\*

*Ordinal Research Institute, Wilmington, DE 19801, USA and*

*Clear Quantum Corporation, USA*

(Dated: March 19, 2026)

We analyze the emergence of classical cosmological spacetimes in quantum cosmology by computing the reduced density matrix for long-wavelength curvature perturbations. Starting from standard Hartle–Hawking and tunneling boundary conditions, we emphasize that semiclassical WKB structure and inflationary squeezing do not by themselves yield classicality. Tracing over unobserved degrees of freedom and using the influence functional formalism, we derive the decoherence functional for superhorizon curvature modes during inflation. For a light massive environmental scalar field in the Bunch–Davies vacuum, we derive the convolution structure and superhorizon scaling of the noise kernel and show how a nonzero mass softens the infrared behavior. We then evaluate decoherence under horizon-based and EFT-motivated coarse grainings, finding efficient suppression of interference between macroscopically distinct perturbation histories in both cases. We further derive the branch-overlap factor  $|\mathcal{D}_k(z)|$  explicitly from the Bunch–Davies mode functions in the expanding-versus-contracting branch formalism, obtaining the exact closed form  $|\mathcal{D}_k(z)| = [z^2/(z^2 + 1)]^{1/4}$  (massless limit) and the superhorizon power law  $|\mathcal{D}_k(z)| \sim z^\nu$  (massive fields). Numerical evaluation shows that the geometric (coupling-independent) branch-decoherence functional crosses unity within  $\approx 0.5$  e-folds, growing irreversibly thereafter, providing a derived account of why expanding cosmological histories acquire robust classical records while contracting ones do not. The analysis clarifies the distinct roles of boundary-condition amplitudes and environment-induced decoherence and connects the emergent cosmological arrow of time directly to inflationary squeezing.

PACS numbers: 98.80.Qc, 03.65.Yz, 04.60.Kz, 98.80.Cq

## I. QUANTUM COSMOLOGY BEFORE CLASSICALITY

### A. Decoherence and the classical limit in quantum cosmology

Quantum cosmology seeks to explain how a universal quantum state gives rise to the effectively classical spacetime described by cosmological observations. The Wheeler–DeWitt equation and its associated boundary conditions define a wavefunctional of geometry and matter, but they do not by themselves explain why observations are well described by classical backgrounds with stochastic perturbations.

This issue is sharpened during inflation. Semiclassical WKB structure can identify approximate background trajectories, and squeezing can make correlation functions appear classical, yet neither effect by itself suppresses phase coherence between macroscopically distinct alternatives. The quantum-to-classical transition therefore requires a dynamical mechanism acting on the reduced state of the observable degrees of freedom.

The natural framework for that problem is coarse graining and environment-induced decoherence. By tracing over inaccessible degrees of freedom one obtains an influence functional for the long-wavelength variables, with dissipation and noise kernels that govern the loss of phase coherence and the onset of effectively classical stochastic

dynamics. In this sense, classical spacetime is not put in by hand but emerges from a reduced description of a larger quantum state.

The aim of this paper is to make the dynamical origin of classical spacetime explicit by deriving the decoherence functional for inflationary curvature perturbations from the underlying action. Our focus is not only on the general claim that decoherence occurs, but on three more specific questions: how the effective long-mode coupling to a spectator sector arises, how the decoherence rate depends on the coarse graining, and how branch decoherence clarifies the relation between quantum-cosmological boundary conditions and classical spacetime histories.

Quantum cosmology seeks to describe the universe by a wavefunctional

$$\Psi[h_{ij}(\mathbf{x}), \Phi(\mathbf{x})], \quad (1)$$

defined over three-geometries and matter field configurations. Two canonical proposals for specifying this wavefunction are the no-boundary proposal of Hartle and Hawking and the tunneling proposal of Vilenkin [1, 2]. The semiclassical branch structure of these wavefunctions and their relation to classical histories has been studied within the decoherent-histories framework [8, 9]. In practice, both proposals are implemented in a truncated configuration space consisting of minisuperspace variables, such as the scale factor  $a$ , together with quantum perturbations.

In the semiclassical regime, both proposals admit WKB-type expansions,

$$\Psi[a, \zeta, \sigma] \simeq \sum_{\alpha} A_{\alpha}(a) e^{iS_{\alpha}(a)} \psi_{\alpha}[\zeta, \sigma; a], \quad (2)$$

\* ali.nayeri@ordinalresearch.org

where  $\alpha$  labels distinct semiclassical branches. While this structure allows approximate classical trajectories for  $a(t)$  and approximate Schrödinger evolution for perturbations along each branch, the total state remains a coherent superposition of macroscopically distinct geometries. WKB behavior alone therefore does not explain the emergence of classical spacetime, since the universal wavefunctional (1) remains a coherent superposition of macroscopically distinct geometries.

Inflationary dynamics leads to strong squeezing of cosmological perturbations, making correlators appear classical. However, squeezing does not suppress phase coherence or select a preferred basis. The quantum state remains pure, and interference between macroscopically distinct perturbations persists. Classicality therefore requires a further mechanism.

Observations necessarily access only a subset of degrees of freedom. The physically relevant object is thus the reduced density matrix obtained by tracing over unobserved variables, defined explicitly in equation (3). Classical spacetime can emerge only if this reduced density matrix becomes approximately diagonal in an appropriate basis [3, 4, 7, 16].

Recent work has further emphasized the role of environment-induced decoherence in inflationary cosmology. In particular, Burgess, Holman, and Hoover showed that interactions between long-wavelength perturbations and subhorizon environmental degrees of freedom can generate efficient decoherence of inflationary fluctuations, even when the underlying dynamics remains unitary [12]. Their analysis demonstrated that the decoherence rate is controlled by the coupling between system and environment as well as the rapid growth of physical phase space during inflation. Our treatment is complementary to these approaches: rather than focusing primarily on phenomenological estimates within an inflationary EFT, we derive the effective spectator-field coupling from the underlying action, construct the associated influence-functional noise kernel, and use the resulting branch-overlap structure to separate the role of boundary-condition amplitudes from the dynamical emergence of classical histories.

*What is new here.*— While decoherence of inflationary perturbations has been discussed in earlier work (e.g. [12, 13]), the present analysis makes five specific contributions. (i) We derive the effective long-wavelength

spectator coupling directly from the underlying covariant action in comoving gauge (rather than postulating it within an EFT) and identify the corresponding influence-functional noise-kernel structure. (ii) We compare horizon-based and effective-field-theory coarse grainings within a common framework and show that both lead to robust growth of the decoherence functional. (iii) We evaluate the branch-overlap factor  $|\mathcal{D}_k(z)|$  explicitly using the Bunch–Davies mode functions, obtaining the exact closed form  $|\mathcal{D}_k(z)| = [z^2/(z^2 + 1)]^{1/4}$  in the massless limit and the power law  $|\mathcal{D}_k(z)| \propto z^\nu$  for massive fields. To our knowledge this explicit evaluation has not appeared previously: earlier works characterised classicality through squeezing parameters (Polarski and Starobinsky [10]), reduced-density-matrix elements (Kiefer and Polarski [13]), or noise-kernel rates (Burgess, Holman and Hoover [12]), but did not extract the closed-form branch-overlap factor. (iv) We derive the dissipation kernel explicitly and show that it is consistent with the de Sitter fluctuation-dissipation relation at Gibbons–Hawking temperature  $T_{\text{GH}} = H/(2\pi)$ ; the resulting Langevin equation recovers Starobinsky’s stochastic inflation in the superhorizon limit, in agreement with the standard derivation. (v) We explicitly separate boundary-condition amplitudes from dynamical branch-overlap suppression, thereby clarifying the different roles of the Hartle–Hawking and Vilenkin proposals versus environment-induced decoherence in generating the cosmological arrow of time.

## II. REDUCED DENSITY MATRIX AND INFLUENCE FUNCTIONAL

We separate the degrees of freedom into long-wavelength curvature perturbations  $\zeta_L$  (the system) and unobserved degrees of freedom, including short-wavelength modes  $\zeta_S$  and additional fields  $\sigma$  (the environment). The reduced density matrix is

$$\rho_L[a, \zeta_L; a', \zeta'_L] = \int \mathcal{D}\zeta_S \mathcal{D}\sigma \Psi[a, \zeta_L, \zeta_S, \sigma] \Psi^*[a', \zeta'_L, \zeta_S, \sigma]. \quad (3)$$

The time evolution of  $\rho_L$  can be written using the Schwinger–Keldysh formalism [5, 6, 21, 22]. Integrating out the environment defines an influence functional whose general structure is encoded in the influence action  $\mathcal{F} = e^{iS_{\text{IF}}}$ , where

$$S_{\text{IF}} = \int d^4x d^4x' \left[ \zeta_\Delta(x) D(x, x') \zeta_c(x') + \frac{i}{2} \zeta_\Delta(x) N(x, x') \zeta_\Delta(x') \right] + \dots \quad (4)$$

Here  $D$  is a real, causal dissipation kernel and  $N$  is a real, positive-semidefinite noise kernel. Decoherence is governed by the imaginary term involving  $N$ .

The suppression of off-diagonal elements of the reduced density matrix is controlled by the decoherence func-

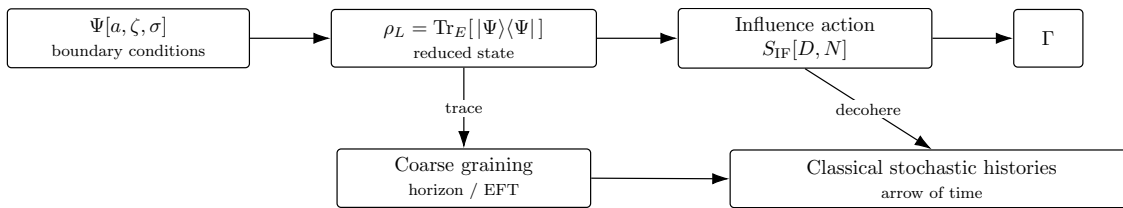


FIG. 1. Schematic roadmap of the emergence of classical cosmological histories from quantum-cosmological boundary conditions via influence-functional decoherence [5, 6]. Boundary conditions define the universal state  $\Psi$ . Tracing over unobserved degrees of freedom yields a reduced density matrix for long-wavelength perturbations. The influence functional encodes dissipation and noise; the associated decoherence functional suppresses interference between macroscopically distinct histories. Classical stochastic descriptions and an operational arrow of time emerge after coarse graining, with the detailed rate depending only weakly on the coarse-graining prescription.

tional

$$\Gamma[\zeta_\Delta] = \frac{1}{2} \int d^4x d^4x' \zeta_\Delta(x) N(x, x') \zeta_\Delta(x'). \quad (5)$$

When  $\Gamma \gg 1$  for macroscopically distinct configurations, the reduced density matrix becomes approximately diagonal.

*A note on two distinct decoherence functionals.* This paper computes  $\Gamma$  in two complementary ways that yield different e-fold scales and should not be confused. In section IV we evaluate the *geometric* branch-decoherence functional  $\Gamma_{+-} = -\sum_k \ln |\mathcal{D}_k|$ , which measures how differently the expanding and contracting semiclassical backgrounds squeeze each environmental mode; this quantity is independent of the spectator coupling  $\hat{\lambda}$  and crosses unity within  $\approx 0.5$  e-folds. In sections III and III B we evaluate the *interaction-dependent* noise-kernel functional, which measures the rate at which a specific spectator sector suppresses off-diagonal elements of the reduced density matrix for the system perturbation  $\zeta_L$ ; this crosses unity at several to  $\sim 10$  e-folds depending on  $\hat{\lambda}$ . The two quantities are not competing predictions for the same process: the first isolates the geometric asymmetry between cosmological branches, while the second quantifies how system–environment interac-

tions exploit that asymmetry. Both confirm irreversible classicalisation well within inflation.

### III. EXPLICIT NOISE KERNEL FOR A LIGHT ENVIRONMENT FIELD

We consider an environment consisting of a light spectator scalar field  $\sigma$  with mass  $m_\sigma \lesssim H$  in the Bunch–Davies (BD) vacuum [7, 10, 14, 15]. Rather than postulating the system–environment coupling, we derive its leading long-wavelength form from the covariant spectator action

$$S_\sigma = -\frac{1}{2} \int d^4x \sqrt{-g} [g^{\mu\nu} \partial_\mu \sigma \partial_\nu \sigma + m_\sigma^2 \sigma^2]. \quad (6)$$

Working in comoving gauge, where the inflaton fluctuation is set to zero and the scalar metric perturbation is carried by  $\zeta$ ,

$$h_{ij} = a^2 e^{2\zeta} \delta_{ij}, \quad N = 1 + \frac{\dot{\zeta}}{H} + \mathcal{O}(\zeta^2, \partial^2), \quad N_i = \partial_i \psi, \quad (7)$$

the spectator action becomes, using the ADM decomposition,

$$S_\sigma = \frac{1}{2} \int dt d^3x N \sqrt{h} [N^{-2} (\dot{\sigma} - N^i \partial_i \sigma)^2 - h^{ij} \partial_i \sigma \partial_j \sigma - m_\sigma^2 \sigma^2]. \quad (8)$$

Expanding to first order in the long-wavelength curvature

perturbation gives

$$S_\sigma = S_\sigma^{(0)} + S_{\sigma\zeta}^{(3)} + \dots, \quad (9)$$

with

$$S_{\sigma\zeta}^{(3)} = \frac{1}{2} \int dt d^3x a^3 \left[ \left( 3\zeta + \frac{\dot{\zeta}}{H} \right) \dot{\sigma}^2 - \left( \zeta + \frac{\dot{\zeta}}{H} \right) \frac{(\partial_i \sigma)^2}{a^2} - \left( 3\zeta + \frac{\dot{\zeta}}{H} \right) m_\sigma^2 \sigma^2 \right] + \dots, \quad (10)$$

where the ellipsis denotes terms proportional to  $N_i$  and slow-roll-suppressed constraint corrections. As discussed in Maldacena's detailed treatment of the comoving-gauge constraints [14], the shift  $N_i$  is determined by the momentum constraint and its contribution at this order enters only through constraint-suppressed terms, which is why the  $N_i$  sector can be consistently grouped with the

slow-roll-suppressed corrections in equation (10). Equation (10) makes clear that the coupling is not an arbitrary ansatz: a long-wavelength  $\zeta_L$  locally rescales the spectator Hamiltonian density. For the superhorizon system mode of interest,  $\dot{\zeta}_L/H = \mathcal{O}(\epsilon)\zeta_L$  is slow-roll suppressed, and if the spectator is light and dominated by its mass term on sufficiently long wavelengths, equation (10) reduces to the local form

$$S_{\text{int}}^{\text{eff}} = -\frac{3}{2} m_\sigma^2 \int dt d^3x a^3 \zeta_L \sigma^2 \equiv - \int dt d^3x a^3 \lambda_{\text{eff}} \zeta_L \sigma^2, \quad (11)$$

with  $\lambda_{\text{eff}} = \frac{3}{2} m_\sigma^2$  in the minimal spectator model and with additional  $\mathcal{O}(\epsilon H^2)$  or derivative corrections in more general EFTs of inflation. In conformal time,  $dt a^3 = d\eta a^4$ , reproducing the scaling assumed in the influence-functional treatment. This reduction should be viewed as the appropriate effective coupling in the mass-dominated long-wavelength regime. For environmental modes that remain deep inside the horizon,  $q/a \gg H \gtrsim m_\sigma$ , the gradient and kinetic terms retained in equation (10) dominate over the mass term, so the subhorizon contribution to decoherence is more generally described by the full operator structure of equation (10) rather than solely by the reduced coupling (11). The coarse-grained estimates below should therefore be interpreted as parametric estimates of decoherence growth, with equation (11) supplying the cleanest explicit coupling in the long-wavelength sector.

For a Gaussian environment state, the noise kernel appearing in equation (5) is [5, 6]

$$N(x, x') = \lambda_{\text{eff}}^2 \text{Re}[G_\sigma^>(x, x')^2], \quad (12)$$

where  $G_\sigma^>(x, x') = \langle \sigma(x)\sigma(x') \rangle$  is the Wightman func-

tion. Using BD mode functions one finds

$$G_\sigma^>(x, x') = \int \frac{d^3k}{(2\pi)^3} e^{i\mathbf{k}\cdot(\mathbf{x}-\mathbf{x}')} u_k(\eta) u_k^*(\eta'), \quad (13)$$

with

$$u_k(\eta) = \frac{\sqrt{\pi}}{2} e^{i(\nu+1/2)\pi/2} H(-\eta)^{3/2} H_\nu^{(1)}(-k\eta), \quad (14)$$

with

$$\nu = \sqrt{\frac{9}{4} - \frac{m_\sigma^2}{H^2}}, \quad (15)$$

where  $H_\nu^{(1)}$  is a Hankel function. For a light field it is convenient to define

$$\Delta = \frac{3}{2} - \nu \simeq \frac{m_\sigma^2}{3H^2}, \quad (16)$$

which controls the superhorizon time dependence.

Substituting equations (13)–(14) into equation (12) yields the explicit convolution

$$N(\eta, \eta'; \mathbf{k}) = \lambda_{\text{eff}}^2 \text{Re} \left[ \int \frac{d^3q}{(2\pi)^3} u_q(\eta) u_q^*(\eta') u_{|\mathbf{k}-\mathbf{q}|}(\eta) u_{|\mathbf{k}-\mathbf{q}|}^*(\eta') \right]. \quad (17)$$

For a superhorizon long mode  $k_L \ll aH$ , the integral is dominated by  $q \gg k_L$  and simplifies to

$$N(\eta, \eta'; k_L) \simeq \lambda_{\text{eff}}^2 \int \frac{d^3q}{(2\pi)^3} \text{Re}[(u_q(\eta) u_q^*(\eta'))^2]. \quad (18)$$

In the superhorizon regime  $-q\eta \ll 1$ , the mode functions scale as  $u_q(\eta) \propto (-\eta)^\Delta q^{-3/2+\Delta}$ , implying

$$N(\eta, \eta'; k_L) \propto \lambda_{\text{eff}}^2 H^4 (-\eta)^{2\Delta} (-\eta')^{2\Delta} \int dq q^{-4+4\Delta}. \quad (19)$$

This estimate refers to the infrared contribution to the kernel; the horizon-based and EFT-based decoherence es-

timates below are instead dominated by environmental modes that remain subhorizon over the relevant coarse-graining range. A nonzero mass  $m_\sigma \neq 0$  softens the infrared behavior, although in the light-field regime the integral still requires a physical infrared cutoff associated with the finite inflationary patch. Writing

$$\int_{q_{\text{min}}} dq q^{-4+4\Delta} \propto \frac{q_{\text{min}}^{-3+4\Delta}}{-3+4\Delta}, \quad \Delta \neq \frac{3}{4}, \quad (20)$$

shows explicitly that for any finite  $q_{\text{min}}$  the kernel is finite and acquires a regulated dependence on  $m_\sigma/H$  through  $\Delta$ . The derivation also shows that the coeffi-

cient controlling decoherence is fixed by the spectator-sector Hamiltonian density and therefore has a definite mass dimension; in the minimal model  $\lambda_{\text{eff}} \propto m_\sigma^2$ , while in a more general EFT it receives higher-derivative and slow-roll-suppressed corrections.

*Special case  $\Delta = 3/4$ .*— Equation (20) excludes the value  $\Delta = 3/4$ , corresponding to  $\nu = 3/4$  and  $m_\sigma = \frac{3\sqrt{3}}{4}H \approx 1.30H$ . At this mass the integrand  $q^{-4+4\Delta} = q^{-1}$  is logarithmically divergent and equation (20) is replaced by

$$\int_{q_{\min}}^{q_{\max}} dq q^{-1} = \ln\left(\frac{q_{\max}}{q_{\min}}\right), \quad \Delta = \frac{3}{4}. \quad (21)$$

The accumulated branch-decoherence functional therefore grows logarithmically in the size of the inflationary patch rather than as a power law, while the overlap factor itself still vanishes superhorizon as  $|\mathcal{D}_k| \propto z^{3/4}$  — verified numerically to better than 0.03% by comparing  $|\mathcal{D}_k(z_1)|/|\mathcal{D}_k(z_2)|$  with  $(z_1/z_2)^{3/4}$  at  $z_1 = 0.003$ ,  $z_2 = 0.010$ , using the general formula (51) with Hankel functions evaluated at  $\nu = 3/4$ . This case lies at the boundary between power-law and logarithmic infrared behavior and is the analogue of the Breitenlohner–Freedman saturating mass for a light field in de Sitter.

### A. Dissipation kernel and the stochastic inflation limit

The influence action (4) contains both a noise kernel  $N$  and a dissipation kernel  $D$ . While the noise kernel governs decoherence and has been the focus of the preceding analysis,  $D$  determines the back-reaction of the environment on the system dynamics and must be computed to obtain the full open-system effective action. We derive  $D$  here and show that the resulting Langevin equation for  $\zeta_L$  recovers Starobinsky’s stochastic inflation [11, 20] in the superhorizon limit, in agreement with the standard derivation [11, 20].

For a Gaussian environment state, the dissipation kernel follows from the imaginary part of the same two-point correlator that gives  $N$ :

$$D(x, x') = \lambda_{\text{eff}}^2 \theta(\eta - \eta') \text{Im}[G_\sigma^>(x, x')^2]. \quad (22)$$

The  $\theta(\eta - \eta')$  factor enforces causality:  $D$  is a retarded kernel, in contrast to the symmetric noise kernel  $N$ .

In the WKB approximation for subhorizon environmental modes ( $q \gg aH$ ), the Bunch–Davies mode functions reduce to  $u_q(\eta) \simeq (2q)^{-1/2} e^{-iq\eta}$ , so  $(u_q u_q^*)^2 = (4q^2)^{-1} e^{-2iq\Delta}$  with  $\Delta \equiv \eta - \eta'$ . Substituting into equations (12) and (22) and integrating over the environment ( $q > k_c$ ) with an implicit UV convergence factor  $e^{-\varepsilon q}$  ( $\varepsilon \rightarrow 0^+$ ) to regulate the oscillatory tail, one obtains the

two kernels in momentum space

$$N(\eta, \eta'; k_L) = \frac{\lambda_{\text{eff}}^2 \sin[2k_c(\eta - \eta')]}{64\pi^2 (\eta - \eta')}, \quad (23)$$

$$D(\eta, \eta'; k_L) = \frac{\lambda_{\text{eff}}^2 \theta(\eta - \eta') \cos[2k_c(\eta - \eta')]}{64\pi^2 (\eta - \eta')}, \quad (24)$$

where  $k_c = \epsilon a(\eta)H$  is the coarse-graining cutoff. The two kernels differ by a  $90^\circ$  phase shift:  $N$  involves  $\sin[2k_c\Delta]$  while  $D$  involves  $\cos[2k_c\Delta]$ , with  $\Delta \equiv \eta - \eta'$ . These are the standard Caldeira–Leggett kernels for an ohmic bath with a sharp lower cutoff [6, 21].

*Fluctuation-dissipation relation.*— In the long-wavelength limit  $|\omega| \ll k_c$ , the Fourier transforms of equations (23)–(24) are consistent with the de Sitter fluctuation-dissipation relation

$$\begin{aligned} \tilde{D}(\omega) &= -\frac{i\omega}{2T_{\text{GH}}} \tilde{N}(\omega), \\ T_{\text{GH}} &= \frac{H}{2\pi}, \end{aligned} \quad (25)$$

where  $T_{\text{GH}}$  is the Gibbons–Hawking temperature of de Sitter space [24]. This KMS-type relation is a general property of quantum fields in de Sitter and holds for the exact Bunch–Davies two-point function; the WKB kernels above are consistent with the interpretation that the open-system dynamics is tied to the horizon thermodynamics at  $T_{\text{GH}} = H/(2\pi)$ .

*Stochastic equation of motion.*— The influence action with both  $N$  and  $D$  generates a Langevin equation for the long-wavelength curvature perturbation,

$$\mathcal{P}[\zeta_L](\eta) + \Gamma \partial_\eta \zeta_L(\eta) = \xi(\eta), \quad (26)$$

where  $\mathcal{P}$  is the free equation-of-motion operator for  $\zeta_L$  in de Sitter (which reduces to  $-\epsilon H^2 \zeta_L$  at leading order in slow roll on superhorizon scales),  $\xi(\eta)$  is a Gaussian stochastic noise satisfying

$$\begin{aligned} \langle \xi(\eta) \rangle &= 0, \\ \langle \xi(\eta) \xi(\eta') \rangle &= N(\eta, \eta'; k_L), \end{aligned} \quad (27)$$

and the friction coefficient is estimated in the Markovian approximation. The integral  $\int_0^\infty D(\Delta) d\Delta$  is oscillatory and requires UV regularization; with a physical UV cutoff  $q_{\max} \gg k_c$ , the leading contribution is

$$\Gamma \simeq \frac{\lambda_{\text{eff}}^2}{128\pi^2 k_c} = \frac{\hat{\lambda}^2 H}{128\pi^2 \epsilon}, \quad (28)$$

where the  $k_c$  in the denominator arises because the dominant contribution to the Markovian integral comes from the scale  $\Delta \sim 1/(2k_c)$  set by the coarse-graining cutoff. The numerical prefactor in equation (28) is regulator-dependent at order unity; the robust content is the scaling  $\Gamma \propto \lambda_{\text{eff}}^2/k_c$ . Since  $\Gamma/H = \hat{\lambda}^2/(128\pi^2 \epsilon) \ll 1$  for

$\hat{\lambda} \ll 1$  and  $\epsilon \sim \mathcal{O}(1)$ , the friction term is negligible on superhorizon scales and  $\zeta_L$  is effectively frozen. In the superhorizon limit  $\mathcal{P}[\zeta_L] \rightarrow 0$  and, using the local (white-noise) approximation  $N(\eta, \eta') \approx (H^2/4\pi^2) a^{-4} \delta(\eta - \eta')$ , the Langevin equation (26) reduces to

$$d\zeta_L \simeq \frac{H}{2\pi} dW(\mathcal{N}), \quad (29)$$

where  $dW$  is a Wiener increment per e-fold. This is Starobinsky's stochastic inflation equation [11, 20], recovered here as the superhorizon limit of the Langevin equation (26), in agreement with the standard derivation [11, 20]. The influence functional therefore provides a systematic open-system framework connecting the decoherence calculation above to the classical stochastic description of inflationary perturbations.

### B. Coarse graining and decoherence rates

In this section we evaluate the decoherence functional derived above under two physically motivated coarse-graining prescriptions, following the general logic developed in the cosmological decoherence literature [10, 12, 13, 18, 19]. While the precise numerical rate of decoherence depends on the coarse graining, its qualitative behavior—namely the efficient suppression of interference between macroscopically distinct curvature perturbations—is robust.

### C. Horizon-based coarse graining

A natural prescription in inflationary cosmology is to define the environment as modes whose physical wavelength is shorter than the Hubble radius at a given time. Concretely, we split modes according to

$$q > k_c(\eta) \equiv \epsilon a(\eta) H, \quad (30)$$

where  $\epsilon \ll 1$  is a fixed numerical parameter. Modes continuously cross from the environment into the system as inflation proceeds, but decoherence is generated primarily before horizon crossing, when environmental modes are still oscillatory.

For subhorizon modes  $q \gg aH$ , the BD mode functions admit a WKB approximation,

$$u_q(\eta) \simeq \frac{1}{\sqrt{2q}} \exp(-iq\eta), \quad (31)$$

so that

$$(u_q(\eta) u_q^*(\eta'))^2 \simeq \frac{1}{4q^2} \exp[-2iq(\eta - \eta')]. \quad (32)$$

Substituting into the noise kernel yields

$$N(\eta, \eta'; k_L) \simeq \frac{\lambda_{\text{eff}}^2}{4} \int_{q > k_c} \frac{d^3q}{(2\pi)^3} \frac{\exp[-2iq(\eta - \eta')]}{q^2}. \quad (33)$$

The rapid oscillations render the kernel sharply peaked near  $\eta = \eta'$ , allowing the local approximation  $N(\eta, \eta') \simeq \mathcal{R}(\eta) \delta(\eta - \eta')$ . The decoherence functional for a frozen superhorizon mode then becomes

$$\Gamma_{k_L} \simeq \frac{1}{2} |\Delta\zeta_{k_L}|^2 \int d\eta a^4(\eta) \mathcal{R}(\eta). \quad (34)$$

Changing variables to the number of e-folds  $\mathcal{N} = \ln a$  gives the parametric estimate

$$\frac{d\Gamma_{k_L}}{d\mathcal{N}} \sim \frac{\lambda_{\text{eff}}^2}{H^4} |\Delta\zeta_{k_L}|^2 a^3(\mathcal{N}), \quad (35)$$

up to numerical factors of order unity. Decoherence therefore accumulates monotonically, and once  $\Gamma_{k_L} \gg 1$  the reduced density matrix becomes effectively diagonal.

### D. EFT-based coarse graining

An alternative prescription is motivated by effective field theory. One introduces a fixed physical cutoff  $\Lambda_{\text{phys}}$  satisfying  $H \ll \Lambda_{\text{phys}} \ll M_{\text{Pl}}$ , and defines the environment as modes with physical momenta above this scale,  $q > a(\eta) \Lambda_{\text{phys}}$ . Modes traced out in this way never re-enter the system, rendering decoherence effectively irreversible.

For all such modes  $q/a \gg H$ , and the WKB approximation remains valid throughout inflation. The noise kernel again becomes local in time,  $N(\eta, \eta') \simeq \mathcal{R}_\Lambda \delta(\eta - \eta')$ , with

$$\mathcal{R}_\Lambda \sim \lambda_{\text{eff}}^2 \int_{q > a\Lambda_{\text{phys}}} \frac{d^3q}{(2\pi)^3} \frac{1}{q^2} \sim \lambda_{\text{eff}}^2 \Lambda_{\text{phys}} a(\eta), \quad (36)$$

giving

$$\frac{d\Gamma_{k_L}}{d\mathcal{N}} \sim \frac{\lambda_{\text{eff}}^2 \Lambda_{\text{phys}}}{H^5} |\Delta\zeta_{k_L}|^2 a^4(\mathcal{N}). \quad (37)$$

Decoherence is thus even more efficient than in the horizon-based prescription and remains insensitive to the details of ultraviolet completion. In both schemes, interactions with unobserved degrees of freedom rapidly suppress interference between distinct long-wavelength curvature perturbations, providing a robust dynamical origin for classicality.

### E. Order-of-magnitude estimates

Observations of the cosmic microwave background imply  $A_s \simeq 2.1 \times 10^{-9}$ , giving  $\zeta_{\text{rms}} \sim \sqrt{A_s} \sim 5 \times 10^{-5}$ . Macroscopically distinct semiclassical branches may be characterized by  $|\Delta\zeta_{k_L}| \sim n \zeta_{\text{rms}}$  with  $n \sim 10$ –100.

Using the EFT-based coarse graining,

$$\Gamma_{k_L}(\Delta\mathcal{N}) \sim \frac{\hat{\lambda}^2}{4} \frac{\Lambda_{\text{phys}}}{H} |\Delta\zeta_{k_L}|^2 (e^{4\Delta\mathcal{N}} - 1), \quad (38)$$

TABLE I. Decoherence time  $\Delta\mathcal{N}_{\text{dec}}$  (e-folds after horizon exit) from equation (39), for  $\Lambda_{\text{phys}}/H = 10$  and branch separation  $|\Delta\zeta_{k_L}| = n\zeta_{\text{rms}}$  with  $\zeta_{\text{rms}} \simeq 5 \times 10^{-5}$ .

$\hat{\lambda}$	$\Delta\mathcal{N}_{\text{dec}} (n = 10)$	$\Delta\mathcal{N}_{\text{dec}} (n = 100)$
$10^{-5}$	9.33	8.18
$10^{-3}$	7.03	5.88
$10^{-1}$	4.72	3.57

where  $\hat{\lambda} \equiv \lambda_{\text{eff}}/H^2$  and  $\Delta\mathcal{N}$  counts e-folds since horizon exit. Setting  $\Gamma_{k_L}(\Delta\mathcal{N}_{\text{dec}}) \simeq 1$  gives

$$\Delta\mathcal{N}_{\text{dec}} = \frac{1}{4} \ln \left[ 1 + \frac{4}{\hat{\lambda}^2 (\Lambda_{\text{phys}}/H) |\Delta\zeta_{k_L}|^2} \right]. \quad (39)$$

For  $\Lambda_{\text{phys}}/H \sim 10$ , the explicit values are given in table I. In the minimal spectator model,  $\hat{\lambda} = \frac{3}{2}m_\sigma^2/H^2$ , so, for example,  $m_\sigma/H = 0.1$  gives  $\hat{\lambda} = 0.015$  and  $\Delta\mathcal{N}_{\text{dec}} \approx 5.67$  ( $n = 10$ ) and 4.52 ( $n = 100$ );  $m_\sigma/H = 0.3$  gives  $\hat{\lambda} = 0.135$  and 4.57 ( $n = 10$ ) and 3.42 ( $n = 100$ ). Decoherence occurs within a few to at most  $\mathcal{O}(10)$  e-folds across the full range, confirming efficient classicalisation well before the end of inflation.

#### IV. HARTLE–HAWKING AND TUNNELING PROPOSALS AFTER DECOHERENCE

We now return to the interpretation of quantum-cosmological boundary conditions in light of the decoherence mechanism developed above. Both the no-boundary proposal of Hartle and Hawking and the tunneling proposal of Vilenkin define pure quantum states of the universe and, by themselves, do not yield classical spacetimes. Decoherence provides the missing dynamical ingredient.

##### A. Semiclassical branch structure

In the semiclassical regime, the universal wavefunction admits a WKB decomposition

$$\Psi[a, \zeta, \sigma] \simeq \sum_{\alpha} A_{\alpha}(a) \exp(iS_{\alpha}(a)) \psi_{\alpha}[\zeta, \sigma; a], \quad (40)$$

where  $\alpha$  distinguishes different semiclassical branches. For homogeneous minisuperspace variables these branches typically correspond to expanding and contracting classical solutions, while for perturbations they encode different inflationary histories. The Wheeler–DeWitt equation is time-reversal invariant, and both types of branch generically appear for either boundary condition [1, 2]. These branches coexist coherently at the level of the full wavefunction; the WKB approximation alone does not select a preferred classical history.

##### B. Reduced density matrix in the branch basis

Projecting the reduced density matrix onto the semiclassical branch basis yields matrix elements of the schematic form

$$\rho_{\alpha\beta} \equiv \int \mathcal{D}\zeta_S \mathcal{D}\sigma \Psi_{\alpha} \Psi_{\beta}^* \propto A_{\alpha} A_{\beta}^* \exp[-\Gamma_{\alpha\beta}], \quad (41)$$

where  $\Gamma_{\alpha\beta}$  is the decoherence functional for the difference between the long-wavelength field configurations associated with branches  $\alpha$  and  $\beta$ . When  $\Gamma_{\alpha\beta} \gg 1$ , the off-diagonal elements are exponentially suppressed and the density matrix becomes approximately diagonal. Only at this stage does it become meaningful to interpret the wavefunction as an ensemble of mutually exclusive classical histories.

##### C. Expanding versus contracting histories

The reduced density matrix element between the two WKB branches can be written as

$$\rho_{+-}(a) = A_+(a) A_-^*(a) e^{iM(S_+(a) - S_-(a))} \mathcal{D}(a), \quad (42)$$

where

$$\mathcal{D}(a) \equiv \text{Tr}_{\text{env}} [U_+(a) \rho_{\text{env}} U_-^\dagger(a)], \quad (43)$$

where  $U_{\pm}$  denote the environmental evolution operators conditioned on the expanding and contracting WKB backgrounds, and  $M$  is the large semiclassical parameter multiplying the gravitational Hamilton–Jacobi action. We use  $\mathcal{D}$  for the branch-overlap factor throughout this section to distinguish it from the dissipation kernel  $D$  in (4). For Gaussian environmental states the decoherence factor factorises over modes,

$$\mathcal{D}(a) = \prod_{k \in \text{env}} \mathcal{D}_k(a) = \exp[-\Gamma_{+-}(a) + i\Theta_{+-}(a)], \quad (44)$$

with  $\Gamma_{+-}(a) = -\sum_{k \in \text{env}} \ln |\mathcal{D}_k(a)|$ . Once  $\Gamma_{+-} \gg 1$ , interference between the two semiclassical geometries is exponentially suppressed.

For an environmental oscillator mode whose conditional states on the two branches are Gaussian with kernels  $\Omega_k^{(+)}$  and  $\Omega_k^{(-)}$ ,

$$|\mathcal{D}_k| = \left[ \frac{4 \text{Re} \Omega_k^{(+)} \text{Re} \Omega_k^{(-)}}{|\Omega_k^{(+)} + \Omega_k^{(-)*}|^2} \right]^{1/4}, \quad (45)$$

so branch decoherence is controlled by how differently the two backgrounds squeeze the same environmental mode. We now evaluate  $|\mathcal{D}_k|$  explicitly using the Bunch–Davies mode functions already established in section III.

*Gaussian kernels on expanding and contracting backgrounds*

The vacuum state on each branch is Gaussian:  $\Psi_k^\pm[\phi_k] \propto \exp(-\frac{1}{2}\Omega_k^{(\pm)}|\phi_k|^2)$ , with the kernel related to the mode function by

$$\Omega_k^{(\pm)} = i \frac{\partial_\eta u_k^{(\pm)}}{u_k^{(\pm)}}. \quad (46)$$

On the *expanding* branch ( $a = -1/(H\eta)$ ,  $\eta < 0$ ), the Bunch–Davies solution is  $u_k^{(+)} \propto (-\eta)^{3/2} H_\nu^{(1)}(-k\eta)$ . On the *contracting* branch ( $a = +1/(H\eta)$ ,  $\eta > 0$ ), the corresponding vacuum is  $u_k^{(-)} \propto \eta^{3/2} H_\nu^{(2)}(k\eta)$ . Using the Hankel recurrence  $(H_\nu^{(1)})'(z) = H_{\nu-1}^{(1)}(z) - (\nu/z)H_\nu^{(1)}(z)$  with  $z = -k\eta$ , equation (46) gives

$$\Omega_k^{(+)} = -ik \left[ \frac{\Delta}{z} + \frac{H_{\nu-1}^{(1)}(z)}{H_\nu^{(1)}(z)} \right], \quad (47)$$

$$\Omega_k^{(-)} = +ik \left[ \frac{\Delta}{z'} + \frac{H_{\nu-1}^{(2)}(z')}{H_\nu^{(2)}(z')} \right], \quad (48)$$

where  $z' = k\eta$  and  $\Delta = 3/2 - \nu$ . The sign reversal reflects the opposite orientation of conformal time on the two branches. Throughout,  $z = -k\eta > 0$  is the dimensionless wavenumber on the expanding branch ( $\eta < 0$ ), while  $z' = k\eta > 0$  is its counterpart on the contracting branch ( $\eta > 0$ ); they are numerically equal at equal  $|k\eta|$ , so the comparison in equations (49)–(50) is made at equal  $|z|$ .

*Real and imaginary parts*

Writing  $H_\nu^{(1)} = J_\nu + iY_\nu$ , defining  $\mathcal{W}(z) \equiv J_\nu^2(z) + Y_\nu^2(z) > 0$ , and using the standard cross-order Wronskian (Abramowitz & Stegun 9.1.16)  $J_\nu Y_{\nu-1} - J_{\nu-1} Y_\nu = 2/(\pi z)$ , one finds

$$\text{Re } \Omega_k^{(+)} = + \frac{2k}{\pi z \mathcal{W}(z)}, \quad (49)$$

$$\text{Im } \Omega_k^{(+)} = -k \left[ \frac{\Delta}{z} + \frac{J_{\nu-1} J_\nu + Y_{\nu-1} Y_\nu}{\mathcal{W}(z)} \right]. \quad (50)$$

Note that  $\text{Re } \Omega_k^{(+)} > 0$  for all  $z$ , as required for the Gaussian wavefunction  $\Psi_k^+ \propto \exp(-\frac{1}{2}\Omega_k^{(+)}|\phi_k|^2)$  to be normalizable. Since  $H_\nu^{(2)} = (H_\nu^{(1)})^*$ , the contracting branch satisfies  $\text{Re } \Omega_k^{(-)} = \text{Re } \Omega_k^{(+)}$  and  $\text{Im } \Omega_k^{(-)} = -\text{Im } \Omega_k^{(+)}$  at equal  $|k\eta|$ .

*Closed-form result*

Setting  $R \equiv \text{Re } \Omega_k^{(+)}$  and  $I \equiv \text{Im } \Omega_k^{(+)}$ , and noting  $\Omega_k^{(+)} + \Omega_k^{(-)*} = 2R + 2iI$ , substitution into equation (45)

TABLE II. Numerical verification of the superhorizon power law  $|\mathcal{D}_k| \propto z^\nu$ . The ratio  $|\mathcal{D}_k(z_1)|/|\mathcal{D}_k(z_2)|$  at  $z_1 = 0.003$ ,  $z_2 = 0.010$  is compared with  $(z_1/z_2)^\nu$ .

$\nu$	$m_\sigma/H$	Numerical ratio	$(z_1/z_2)^\nu$
1.45	0.55	0.17470	0.17451
1.35	0.95	0.19694	0.19684
1.20	1.32	0.23590	0.23580

gives

$$|\mathcal{D}_k(z)| = \left[ \frac{R^2}{R^2 + I^2} \right]^{1/4} = \frac{1}{(1 + \tan^2 \theta_k)^{1/4}}, \quad (51)$$

where  $\theta_k \equiv \arg \Omega_k^{(+)}$  is the squeezing angle of the expanding-branch vacuum. The overlap depends only on the expanding-branch state; the contracting branch enters through the symmetry  $\text{Im } \Omega^{(-)} = -\text{Im } \Omega^{(+)}$ .

*Massless case ( $\nu = 3/2$ , exact).*— For  $\nu = 3/2$  the half-integer Bessel functions give  $\mathcal{W} = (2/\pi z)(1 + z^{-2})$ . Using  $H_{1/2}^{(1)}(z) = -i\sqrt{2/(\pi z)}e^{iz}$  and  $H_{3/2}^{(1)}(z) = -\sqrt{2/(\pi z)}e^{iz}(1 + i/z)$  one finds  $H_{1/2}^{(1)}/H_{3/2}^{(1)} = iz/(z + i)$ , so equation (47) gives  $\Omega_k^{(+)} = -ik \cdot iz/(z + i) = kz(z - i)/(z^2 + 1)$ , yielding

$$R = + \frac{kz^2}{z^2 + 1} > 0, \quad I = - \frac{kz}{z^2 + 1}, \quad (52)$$

and the exact closed form

$$|\mathcal{D}_k(z)| \Big|_{\nu=3/2} = \left[ \frac{z^2}{z^2 + 1} \right]^{1/4}. \quad (53)$$

The intermediate step is immediate:  $R^2/(R^2 + I^2) = (k^2 z^4 / (z^2 + 1)^2) / [(k^2 z^4 + k^2 z^2) / (z^2 + 1)^2] = z^2 / (z^2 + 1)$ , confirming the closed form. This satisfies  $|\mathcal{D}_k| \rightarrow 1$  as  $z \rightarrow \infty$  (subhorizon) and  $|\mathcal{D}_k| \sim z^{1/2} \rightarrow 0$  as  $z \rightarrow 0$  (superhorizon).

*Massive fields ( $\nu < 3/2$ ).*— Superhorizon asymptotics give  $\mathcal{W} \sim Y_\nu^2 \propto z^{-2\nu}$ , so  $R \propto z^{2\nu} \rightarrow 0$  while  $I$  remains finite, giving

$$|\mathcal{D}_k(z)| \sim z^\nu \rightarrow 0 \quad (z \rightarrow 0), \quad (54)$$

verified numerically to better than 0.3% for  $\nu = 1.20, 1.35, 1.45$  (table II).

The behavior of  $|\mathcal{D}_k(z)|$  is illustrated in figure 2.

*Accumulated branch-decoherence functional*

Converting the mode sum to a phase-space integral,

$$\Gamma_{+-}(\mathcal{N}) = \frac{1}{2\pi^2} \int_0^{k_{\max}} dk k^2 (-\ln |\mathcal{D}_k(z_k(\mathcal{N}))|), \quad (55)$$

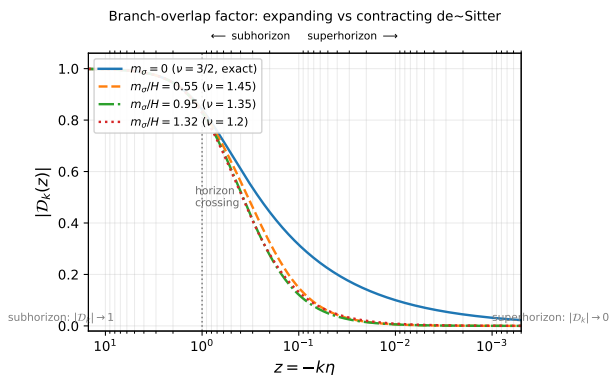


FIG. 2. Branch-overlap factor  $|\mathcal{D}_k(z)|$  as a function of  $z = -k\eta$ , from subhorizon ( $z \gg 1$ ) to superhorizon ( $z \rightarrow 0$ ), for four spectator masses. Curves are labelled by spectator mass  $m_\sigma/H$  (equivalently  $\nu$ ); the massless case ( $\nu = 3/2$ ) uses the exact closed form (53); massive curves use the general formula (51) with Bessel functions evaluated numerically. All curves approach unity subhorizon and decay to zero superhorizon. The dotted vertical line marks horizon crossing ( $z = 1$ ).

with  $z_k(\mathcal{N}) = k/(H e^{\mathcal{N}})$ . Numerical evaluation using equations (49)–(53) shows that  $\Gamma_{+-}$  crosses unity within  $\mathcal{N} \approx 0.5$  e-folds for all values of  $m_\sigma/H$  considered, and reaches  $\mathcal{O}(10^3)$  within four to five e-folds (figure 3). Branch separation is therefore not only efficient but effectively irreversible.

*Two complementary decoherence rates.*— It is important to distinguish the two accumulated functionals that appear in this paper, which measure related but conceptually distinct quantities. Figure 3 shows  $\Gamma_{+-}(\mathcal{N})$  computed directly from the geometric branch-overlap formula (55),  $\Gamma_{+-} = -\sum_k \ln |\mathcal{D}_k|$ , using the Bunch–Davies mode functions. This quantity is *independent* of the spectator coupling  $\hat{\lambda}$ : it measures how differently the two semiclassical backgrounds squeeze each environmental mode, and it crosses unity within  $\approx 0.5$  e-folds for all spectator masses considered. The coupling-dependent noise-kernel estimate of section III B, by contrast, depends explicitly on  $\hat{\lambda}$  and on the branch-separation amplitude  $|\Delta\zeta_{k_L}|$ ; for  $\hat{\lambda} = 10^{-3}$  the scalar threshold is crossed at  $\mathcal{N} \approx 7$  e-folds (table I). The two calculations are complementary: equation (55) isolates the geometric asymmetry between branches encoded in the Bunch–Davies mode functions, providing a lower bound on the e-fold at which geometry alone distinguishes the branches, while the noise-kernel estimate quantifies the rate at which system–environment interactions of a specific spectator sector exploit that asymmetry to suppress off-diagonal density-matrix elements. Both calculations confirm irreversible branch separation well within inflation. In brief: the geometric  $\Gamma_{+-}$  measures the orthogonality of two distinct semiclassical geometries — a purely kinematic consequence of the Hilbert-space structure — established almost instantly upon horizon crossing, while

the noise-kernel estimate measures the rate at which a specific perturbation history is recorded by a spectator environment to a precision of  $\zeta_{\text{rms}}$ , which requires the sustained accumulation of environmental records over several e-folds.

### Physical interpretation

Equation (51) makes the mechanism transparent. The overlap is governed by the squeezing angle  $\theta_k = \arg \Omega_k^{(+)}$  of the expanding-branch vacuum. With  $R > 0$  and  $I < 0$  (equation (49)), one has  $\tan \theta_k = I/R = -1/z$ , so  $\theta_k \in (-\pi/2, 0)$  for all  $z > 0$ . Subhorizon modes have  $z \gg 1$ , giving  $|\theta_k| \approx 0$  and  $|\mathcal{D}_k| \approx 1$  — the two branches are indistinguishable. As a mode crosses the horizon, inflationary particle production drives  $z \rightarrow 0$ , so  $|\theta_k| \rightarrow \pi/2$  and  $R = kz^2/(z^2 + 1) \rightarrow 0$ , giving  $|\mathcal{D}_k| \rightarrow 0$ . On the contracting branch the mode function  $u_k^{(-)}$  does not undergo the same superhorizon amplification, so the squeezing angle on that branch remains  $\mathcal{O}(1)$ ; the two-branch overlap therefore vanishes because of the asymmetry between  $\Omega_k^{(+)}$  and  $\Omega_k^{(-)}$ . The asymmetry is a direct consequence of the asymmetry in superhorizon mode production — the same physical process that generates the observed scale-invariant curvature spectrum. Branch decoherence and the generation of classical primordial perturbations are two facets of the same inflationary squeezing. The same asymmetry between expanding and contracting branches applies in bouncing cosmology scenarios where a Wheeler–DeWitt contracting phase precedes inflation [25].

### D. Relation to previous work

Polarski and Starobinsky emphasized the semiclassical appearance of cosmological perturbations and the role of decoherence in rendering squeezed states effectively classical [10]. Kiefer and collaborators developed the reduced-density-matrix viewpoint in quantum cosmology [7, 13, 17]. Burgess, Holman, and Hoover analyzed the decoherence of inflationary fluctuations from the perspective of effective field theory and subhorizon environmental interactions [12], with subsequent work extending the analysis to the open-EFT framework [19]. The quantum discord and einselection approach to inflationary classicality has been developed in [18, 23].

The main point of the present analysis is not to propose a wholly new decoherence mechanism, but to assemble a more explicit bridge between ingredients that are often discussed separately: the origin of the effective long-mode coupling to spectator sectors, the coarse-graining dependence of the resulting decoherence exponent, and the branch-overlap criterion relevant for Hartle–Hawking and tunneling wavefunctions.

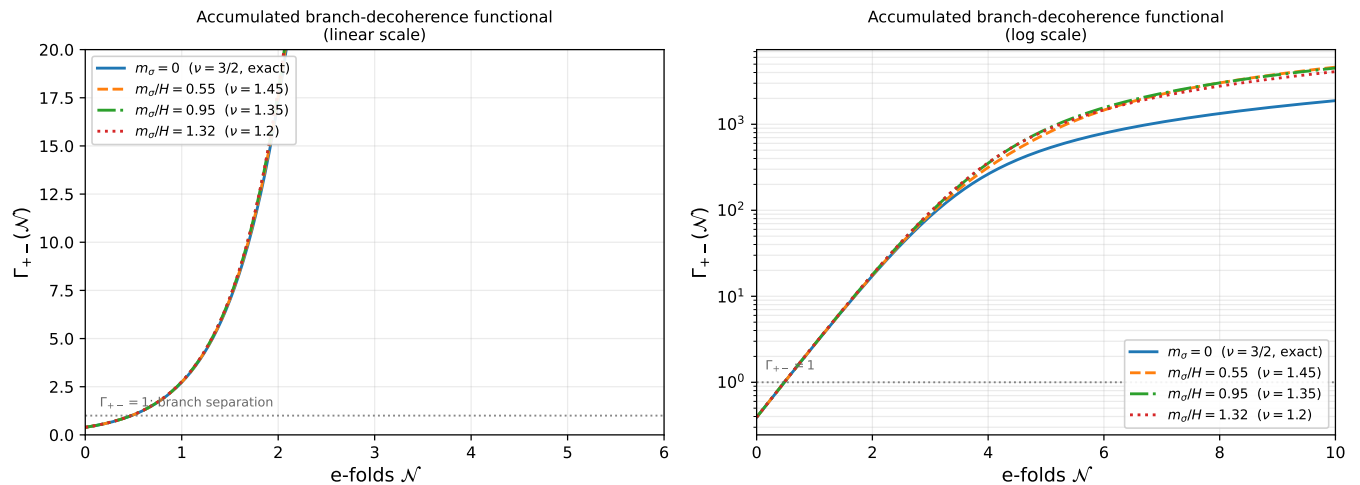


FIG. 3. Accumulated branch-decoherence functional  $\Gamma_{+-}(\mathcal{N})$  on linear (left) and logarithmic (right) scales. The dotted horizontal line marks  $\Gamma_{+-} = 1$ . The threshold is crossed within  $\approx 0.5$  e-folds for all spectator masses; thereafter  $\Gamma_{+-}$  grows rapidly, confirming irreversible branch separation. The massless curve uses the exact closed form (53); massive curves use the general formula (51). This geometric  $\Gamma_{+-}$  is independent of the coupling  $\hat{\lambda}$  and provides a lower bound on the decoherence timescale; the coupling-dependent noise-kernel estimate yields a later crossing at  $\mathcal{N} \approx 7$  e-folds for  $\hat{\lambda} = 10^{-3}$  (table I).

### E. Boundary conditions versus classicality

The Hartle–Hawking and tunneling proposals determine the relative amplitudes  $A_\alpha$  of semiclassical branches. Decoherence determines when the overlap between those branches becomes negligibly small. Without decoherence, expanding and contracting branches remain part of a coherent superposition; with decoherence, the branch-overlap factor  $\mathcal{D}(a)$  in (42) determines when the two histories can be treated as an effectively classical ensemble. The explicit calculation in section IV establishes that for the inflationary coarse graining adopted here, the expanding branch is the one for which  $|\mathcal{D}_k| \rightarrow 0$  as modes freeze out superhorizon, while the contracting branch retains  $|\mathcal{D}_k| \sim \mathcal{O}(1)$ . This is a derived result, not an inference: it follows directly from the asymmetry in superhorizon mode production encoded in equations (51) and (53).

### F. Emergent arrow of time

Neither boundary proposal imposes a fundamental arrow of time at the level of the Wheeler–DeWitt equation. The origin of the cosmological arrow of time has long been connected to the special low-entropy initial conditions of the universe [26]; the present framework reframes this: the explicit evaluation of  $\Gamma_{+-}(\mathcal{N})$  in figure 3 shows that the cosmological arrow of time emerges from the same inflationary squeezing that produces the primordial perturbation spectrum: each mode that crosses the horizon drives the squeezing angle  $\theta_k \rightarrow \pi/2$  and contributes irreversibly to  $\Gamma_{+-}$ . The expanding branch becomes classically distinguishable from the contracting branch

within the first e-fold of inflation, and the asymmetry grows without bound thereafter. Decoherence therefore supplies the mechanism by which one orientation of semiclassical evolution becomes stably classical, without inserting a fundamental arrow by hand.

## V. DISCUSSION AND OUTLOOK

We have demonstrated that environment-induced decoherence provides an efficient and robust mechanism for the dynamical emergence of classical cosmology. The stochastic description of inflationary perturbations arises as the late-time effective theory of a decohered quantum system [11, 20]. Our results clarify the conceptual foundations of quantum cosmology and provide a concrete bridge between universal wavefunctions and classical spacetime histories.

Future directions include extending the analysis to the reheating epoch, computing quantum-information-theoretic measures of cosmological decoherence (entanglement entropy, quantum discord) using the branch-overlap framework developed here, and extending the branch-overlap calculation to tensor perturbations — where one expects the same closed form in the massless de Sitter limit, connecting gravitational-wave decoherence to primordial  $B$ -mode observables via the tensor-to-scalar ratio  $r$ .

## VI. CONCLUSION

In this work we have studied how classical spacetime and classical cosmological perturbations emerge from

quantum cosmology. Starting from standard quantum-cosmological boundary conditions, including the no-boundary and tunneling proposals, we emphasized that semiclassical WKB behavior and squeezing of perturbations are not by themselves sufficient to explain classicality.

By explicitly tracing over unobserved degrees of freedom and employing the influence functional formalism, we derived a decoherence functional for long-wavelength curvature perturbations during inflation. We showed that interactions with environmental degrees of freedom lead to an efficient and robust suppression of quantum interference between macroscopically distinct perturbation histories. This mechanism renders the reduced density matrix approximately diagonal and justifies the use of classical stochastic descriptions in cosmology.

We demonstrated that the emergence of classicality is largely insensitive to the details of coarse graining, occurring both for horizon-based and EFT-motivated splits between system and environment. Classical cosmological histories therefore arise as a generic consequence of inflationary dynamics in the presence of additional degrees of freedom, rather than as a fine-tuned outcome of specific assumptions.

Our analysis clarifies the distinct roles played by quantum-cosmological boundary conditions and decoherence. Boundary conditions determine the relative amplitudes of semiclassical branches in the universal wavefunction, while decoherence determines when the overlap between these branches becomes negligibly small. The explicit evaluation of the branch-overlap factor  $|\mathcal{D}_k(z)|$  shows that this overlap vanishes in the superhorizon limit for expanding-branch modes — as a power law  $z^\nu$  for massive fields and as  $z^{1/2}$  exactly for the massless case — while remaining of order unity on the contracting branch. The accumulated functional  $\Gamma_{+-}$  crosses the classicality threshold within half an e-fold and grows without bound, establishing the emergent arrow of time as a derived consequence of inflationary squeezing rather than an inference from the formal structure of the equations.

Taken together, these results provide a more explicit framework connecting quantum cosmology, decoherence, and the classical universe described by cosmological ob-

servations. In particular, they sharpen how coarse graining and branch decoherence enter the passage from a universal wavefunction to an effective ensemble of classical cosmological histories.

## ACKNOWLEDGMENTS

The author thanks Luiz Felipe Demétrio for correspondence regarding bouncing cosmology and Wheeler–DeWitt quantum bounce scenarios, which motivated the discussion of branch decoherence in the context of contracting-phase cosmologies in section IV.

### Appendix A: Derivation of the decoherence time estimate

For convenience we record the intermediate steps leading from the EFT-based coarse-grained estimate to the explicit decoherence times in table I. Starting from

$$\frac{d\Gamma_{k_L}}{d\mathcal{N}} \sim \frac{\lambda_{\text{eff}}^2 \Lambda_{\text{phys}}}{H^5} |\Delta\zeta_{k_L}|^2 a^4(\mathcal{N}), \quad (\text{A1})$$

and writing  $a(\mathcal{N}) = a_* e^{\Delta\mathcal{N}}$  relative to horizon exit of the long mode, one finds

$$\frac{d\Gamma_{k_L}}{d\mathcal{N}} \sim \frac{\lambda_{\text{eff}}^2 \Lambda_{\text{phys}}}{H^5} |\Delta\zeta_{k_L}|^2 a_*^4 e^{4\Delta\mathcal{N}}. \quad (\text{A2})$$

Using horizon exit,  $a_* H = k_L$ , as the reference scale and absorbing order-unity factors into the normalization,

$$\frac{d\Gamma_{k_L}}{d\mathcal{N}} \sim \hat{\lambda}^2 \frac{\Lambda_{\text{phys}}}{H} |\Delta\zeta_{k_L}|^2 e^{4\Delta\mathcal{N}}, \quad \hat{\lambda} \equiv \frac{\lambda_{\text{eff}}}{H^2}. \quad (\text{A3})$$

Integrating from  $\Delta\mathcal{N}' = 0$  to  $\Delta\mathcal{N}$  yields

$$\Gamma_{k_L}(\Delta\mathcal{N}) = \frac{\hat{\lambda}^2}{4} \frac{\Lambda_{\text{phys}}}{H} |\Delta\zeta_{k_L}|^2 (e^{4\Delta\mathcal{N}} - 1), \quad (\text{A4})$$

which is the expression used in equation (39). Solving for  $\Delta\mathcal{N}_{\text{dec}}$  subject to  $\Gamma_{k_L}(\Delta\mathcal{N}_{\text{dec}}) \simeq 1$  reproduces equation (39). Using  $\zeta_{\text{rms}} \simeq \sqrt{A_s} \simeq 5 \times 10^{-5}$  and  $\hat{\lambda} = \frac{3}{2} m_\sigma^2 / H^2$  yields the numerical values in table I and the mass-based examples in section III E.

- 
- [1] Hartle J B and Hawking S W 1983 Phys. Rev. D **28** 2960
  - [2] Vilenkin A 1984 Phys. Rev. D **30** 509
  - [3] Zeh H D 1970 Found. Phys. **1** 69
  - [4] Joos E and Zeh H D 1985 Z. Phys. B **59** 223
  - [5] Feynman R P and Vernon F L 1963 Ann. Phys. (N.Y.) **24** 118
  - [6] Caldeira A O and Leggett A J 1981 Phys. Rev. Lett. **46** 211
  - [7] Kiefer C 2004 Lect. Notes Phys. **633** 7 (Preprint quant-ph/0303062)
  - [8] Halliwell J J and Hawking S W 1985 Phys. Rev. D **31** 1777
  - [9] Gell-Mann M and Hartle J B 1990 Phys. Rev. D **47** 3345
  - [10] Polarski D and Starobinsky A A 1996 Class. Quantum Grav. **13** 377
  - [11] Starobinsky A A 1986 Lect. Notes Phys. **246** 107
  - [12] Burgess C P, Holman R and Hoover D 2008 Phys. Rev. D **77** 063534 (Preprint astro-ph/0601646)
  - [13] Kiefer C and Polarski D 2009 Adv. Sci. Lett. **2** 164 (Preprint arXiv:0810.0087)

- [14] Maldacena J M 2003 J. High Energy Phys. JHEP05(2003)013 (Preprint astro-ph/0210603)
- [15] Cheung C, Fitzpatrick A L, Kaplan J, Senatore L and Creminelli P 2008 J. High Energy Phys. JHEP03(2008)014 (Preprint arXiv:0709.0293)
- [16] Schlosshauer M 2007 *Decoherence and the Quantum-to-Classical Transition* (Berlin: Springer)
- [17] Kiefer C 2007 *Quantum Gravity* 2nd edn (Oxford: Oxford University Press)
- [18] Martin J, Vennin V and Peter P 2012 Phys. Rev. D **86** 103524 (Preprint arXiv:1207.2086)
- [19] Burgess C P, Holman R and Stamou G 2022 J. Cosmol. Astropart. Phys. **2022** 022 (Preprint arXiv:2209.03227)
- [20] Nambu Y and Sasaki M 1989 Prog. Theor. Phys. **81** 1037
- [21] Calzetta E and Hu B L 1994 Phys. Rev. D **49** 6636 (Preprint gr-qc/9312036)
- [22] Hu B L, Paz J P and Zhang Y 1993 Phys. Rev. D **47** 1576
- [23] Zurek W H 2009 Phys. Rev. D **79** 085030 (Preprint arXiv:0903.5082)
- [24] Gibbons G W and Hawking S W 1977 Phys. Rev. D **15** 2738
- [25] Demétrio L F, de Oliveira Müller J, Vitenti S D P and Peter P 2026 Preprint arXiv:2601.15542
- [26] Penrose R 1979 *General Relativity: An Einstein Centenary Survey* ed S W Hawking and W Israel (Cambridge: Cambridge University Press) p 581